



# Temperature Variations of a Geomembrane Liner in a Municipal Solid Waste Landfill from Construction to Closure

Abdelmalek Bouazza<sup>1\*</sup> and Lu Zhang<sup>1,2</sup>

**Abstract** | This paper explores the variations of the temperatures of a black high-density polyethylene (HDPE) geomembrane (GMB) liner in a municipal solid waste landfill through the lens of a field case study. The geomembrane temperature was monitored from the start of the construction phase to the closure phase, a span of 7 years. Solar radiation had a significant effect on the temperature variations of the geomembrane while exposed to the atmosphere. The more significant impact was on the geomembrane on the side slope of the cell, where temperatures were much higher than on the cell floor. A white geotextile cushion did not insulate the geomembrane from solar radiation, which still experienced elevated temperatures. However, the placement of the drainage layer reduced the impact of solar radiation on the GMB and insulated it. The daily temperature variation of the geomembrane covered with a white geotextile varied from 12 °C to 38 °C at floor level but dropped to 20 °C after the placement of the drainage layer. Along the side slope, without the drainage layer, the daily temperature variation of the GMB fluctuated between 5 and 59 °C and dropped to 23 °C after the installation of the drainage layer.

## 1 Introduction

Hydraulic barrier systems of modern landfills are typically composed of clay-based materials and geosynthetics such as geomembranes and geosynthetic clay liners to isolate waste from the surrounding environment<sup>4–7, 19, 30, 31, 35, 36</sup>. Geomembranes (GMBs) act primarily as isolation layers to minimise contaminants' possible migration and form composite liners when combined with geosynthetic clay liners or compacted clay liners. These composite liners are often exposed to elevated temperatures during construction and operation processes<sup>8–11, 13, 18, 19, 20, 21, 26, 29</sup>, primarily due to exposure to diurnal temperatures during the construction phase, nature of the waste and waste biological decomposition during operation and after closure. These high temperatures can significantly impact the service life of the geosynthetics components of engineered lining

systems<sup>26</sup>. As a basic concept, an engineered component's service life can be considered the period that it continues to meet its design function.

Yesiller and Hanson<sup>32</sup> reported that the temperature of an uncovered geomembrane at a municipal solid waste landfill fluctuated with seasonal air temperatures, which varied approximately between – 10 and 35 °C. Once the GMB was covered by waste, its temperature became steady and gradually increased from 13 °C (ambient temperature) to approximately 28 °C (the ambient temperature was then about 15 °C) within 5 years. Furthermore, Rowe et al.<sup>25</sup> indicated that the surface temperature of an exposed GMB was much higher than either soil or ambient temperature throughout most of the days. This is because the GMB surface temperature is strongly related to solar energy input<sup>25, 28</sup>. The field study reported by Rowe et al.<sup>25</sup> showed that

<sup>1</sup> Department of Civil Engineering, Monash University, 23 College Walk, Clayton, VIC 3800, Australia.

<sup>2</sup> Geosciences & Environment Business Unit, Cardno Victoria Pty Ltd, Melbourne, VIC 3000, Australia.

\*malek.bouazza@monash.edu

as the solar radiation was less than  $50 \text{ W/m}^2$ , the GMB surface temperature was similar to the ambient temperature of  $2 \text{ }^\circ\text{C}$ ; as the solar radiation increased to  $600 \text{ W/m}^2$ , the GMB temperature increased to  $36 \text{ }^\circ\text{C}$  with ambient temperature increasing to  $13 \text{ }^\circ\text{C}$ .

Although many researchers have examined temperature effects on waste containment liners<sup>1, 2, 9–11, 13, 14, 16, 17, 18, 21, 22, 25, 27, 28, 32, 33</sup>, there is still a paucity of data available on temperature variations on a GMB from construction to closure. This paper examines the temperature range experienced by a black HDPE GMB liner installed in a landfill located in Melbourne East, Australia, from construction to closure. The effects of solar

radiation, ambient temperature, protection layer and operational conditions on the GMB temperature are presented and discussed. The exposed GMB temperature recorded in-situ is compared with the theoretical GMB temperature obtained from a heat balance model. Finally, a solar radiation coefficient for a black GMB covered by a white geotextile is derived based on theoretical values and current field data.

## 2 Site

The Geographical Information System (GIS) coordinates of the site centroid in longitude and latitude (decimal degrees) coordinates in the

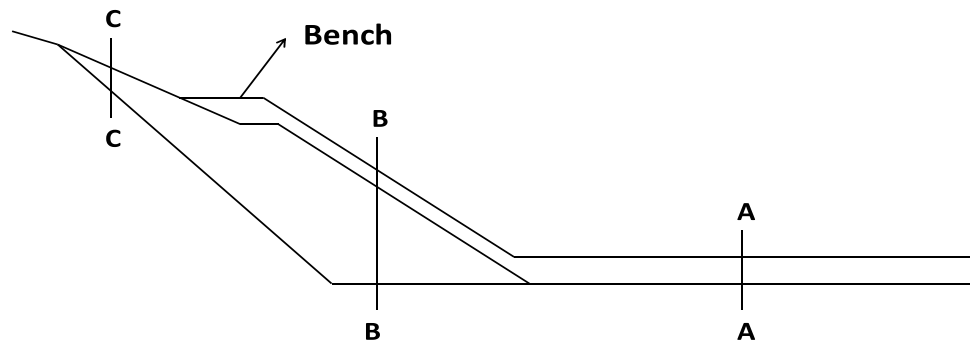


**Figure 1:** Schematic cross sectional view of the side of the landfill cell.

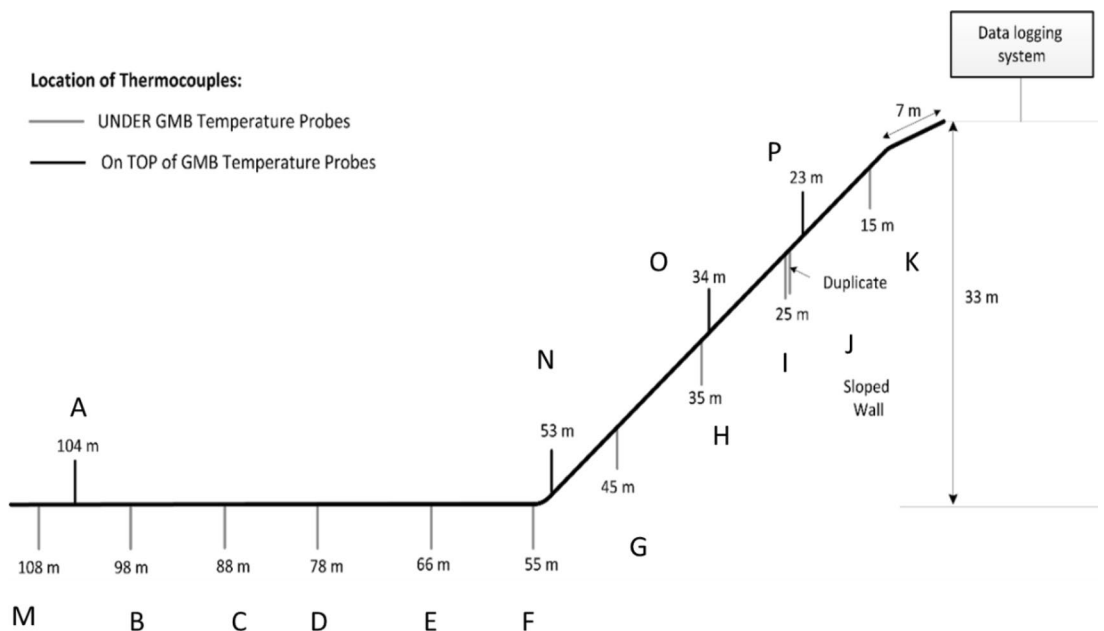


**Figure 2:** Locations of temperature sensors on site (the numbers represent cable length from the slope crest) Note: drawing is not to scale.

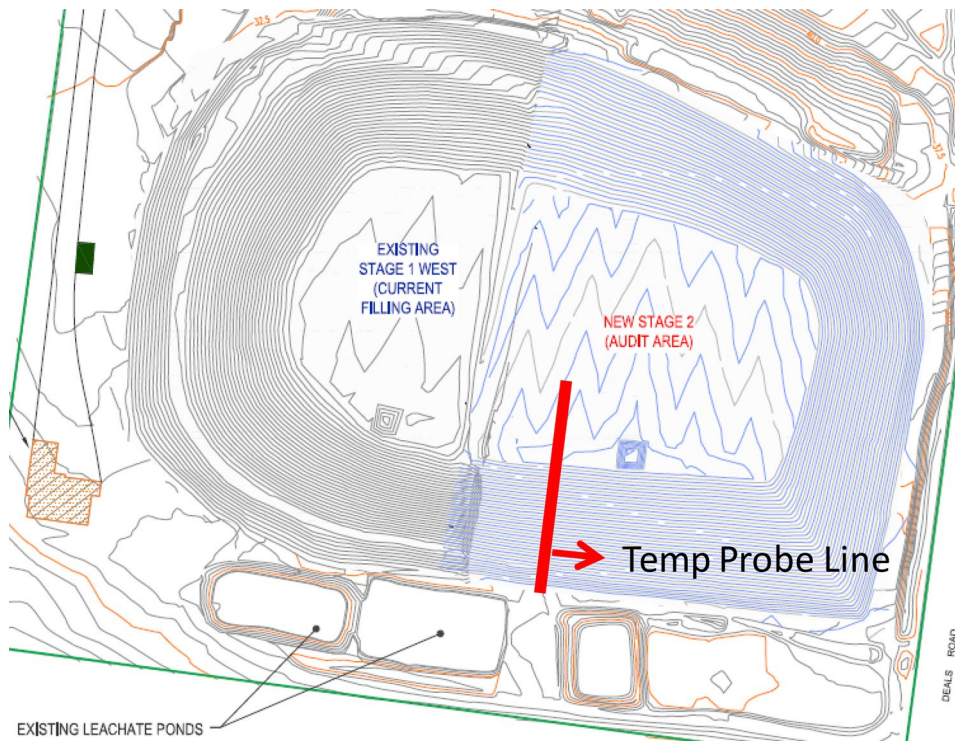


**Figure 3:** Indicative locations of the temperature probes on site.

**Table 1:** Summary of temperature and moisture probes location.

Cable no	Cable length to the crest (m)	Location
A	108	Under GMB Floor
M	104	On top of GMB Floor
B	98	Under GMB Floor
C	88	Under GMB Floor
D	78	Under GMB Floor
E	66	Under GMB Floor
F	55	Under GMB Wall
N	53	On top of GMB Wall
G	45	Under GMB Wall
H	35	Under GMB Wall
O	34	On top of GMB Wall
I	25	Under GMB Wall
J	25	Under GMB Wall
P	23	On top of GMB Wall
K	15	Under GMB Wall

and one in the southern part. The north pit was developed into three landfill cells, whilst the southern pit was divided into two landfill stages. Landfilling of waste in the northern pit ceased in 2003. Since the operations began, it accepted 2.8 million tonnes of waste comprising municipal solid waste from garbage collection (54.9%), construction and industrial waste (14.8%), construction and demolition waste (3.8%) and fills (26.4%).

The monitoring area was located in Stage 2 of the southern pit. The base footprint of Stage 2 is approximately 1.3 ha. The cell was designed to provide approximately 1,000,000 m<sup>3</sup> of air-space when combined with the remaining Stage 1 filling area<sup>15</sup>. The landfill site (located in Melbourne) lies within the Southern Hemisphere. The Southern Hemisphere seasons are reversed to those in Europe, North America and most of Asia. The summer season is from December to February, with temperature ranging from 14 to 45 °C (BOM, 2016), whilst the average local rainfall is about 48 mm<sup>3</sup>. The Winter season is from June to August, and the temperature fluctuates between 6 and 15 °C<sup>3</sup> with average local rainfall of about 49 mm<sup>3</sup>.

The schematic cross-section of the side of the cell, which was monitored, is shown in Fig. 1.

1994 Geocentric Datum of Australia (GDA94) is 145.116735 E and 37.953165 S, respectively<sup>15</sup>. The site was previously quarried for sand, creating one pit in the northern part of the quarry



**Figure 4:** A temperature probe being installed in an HDPE pocket beneath the GMB liner above the compacted clay liner at the floor level (left) welding of an HDPE pocket for a temperature probe above the GMB liner at the floor level (right).

**Table 2:** Recorded maximum and minimum geomembrane temperatures from 2009 to 2017.

Sensors	Cable length (m)	Max temp (°C)	Recorded max time	Min temp (°C)	Recorded min time
Air °C	N/A	44	1/17/2014 15:00	0	7/20/2015 6:00
A °C	108	35	11/24/2009 13:00	14	12/1/2009 5:00
B °C	98	38	11/24/2009 13:00	14	12/1/2009 5:00
C °C	88	37	11/24/2009 13:00	13	12/1/2009 5:00
D °C	78	37	11/24/2009 14:00	14	12/1/2009 5:00
E °C	66	34	1/11/2010 14:00	8	4/16/2012 7:00
F °C	55	58	1/11/2010 13:00	10	3/31/2010 6:00
G °C	45	55	2/3/2010 12:00	5	6/22/2010 5:00
H °C	35	54	2/3/2010 13:00	3	8/25/2010 4:00
I °C	25	55	2/3/2010 13:00	4	8/25/2010 6:00
J °C	25	59	2/3/2010 13:00	4	8/25/2010 6:00
K °C	15	52	2/3/2010 13:00	4	7/16/2011 8:00
M °C	104	32	11/24/2009 13:00	15	12/1/2009 5:00
N °C	53	54	1/11/2010 14:00	8	5/1/2010 1:00
O °C	34	53	2/3/2010 13:00	5	7/9/2010 8:00
P °C	23	53	2/3/2010 13:00	5	7/9/2010 8:00

The format of the time is month/day/year and hh: mm

At the floor level, which is denoted as AA in Fig. 1, the liner system consisted, from bottom to top, of 1 m compacted clay liner sitting above a subgrade, a 1.5 mm thick HDPE GMB, a geotextile cushion to protect the GMB from potential sharp objects, a drainage layer with pipes to collect the leachate generated, and finally a filtration/separation geotextile. Below the bench above the floor, denoted as BB in Fig. 1, the liner system consisted from bottom to top of underdrains (wall drains), engineering fill to shape the 3H:1 V

side slope, followed by a 1 m thick compacted clay liner (CCL), a 1.5 mm smooth HDPE GMB and a geotextile cushion layer (mass per unit area,  $M_A = 700 \text{ g/m}^2$ ). Above the bench, denoted as CC in Fig. 1, the liner system consisted from bottom to top of a layer of underdrains, engineering fill to shape the 3H:1 V side slope, a geosynthetic clay liner (GCL), and a 1.5 mm textured HDPE GMB covered by a cushion geotextile (mass per unit area,  $M_A = 500 \text{ g/m}^2$ ). It should be noted that a

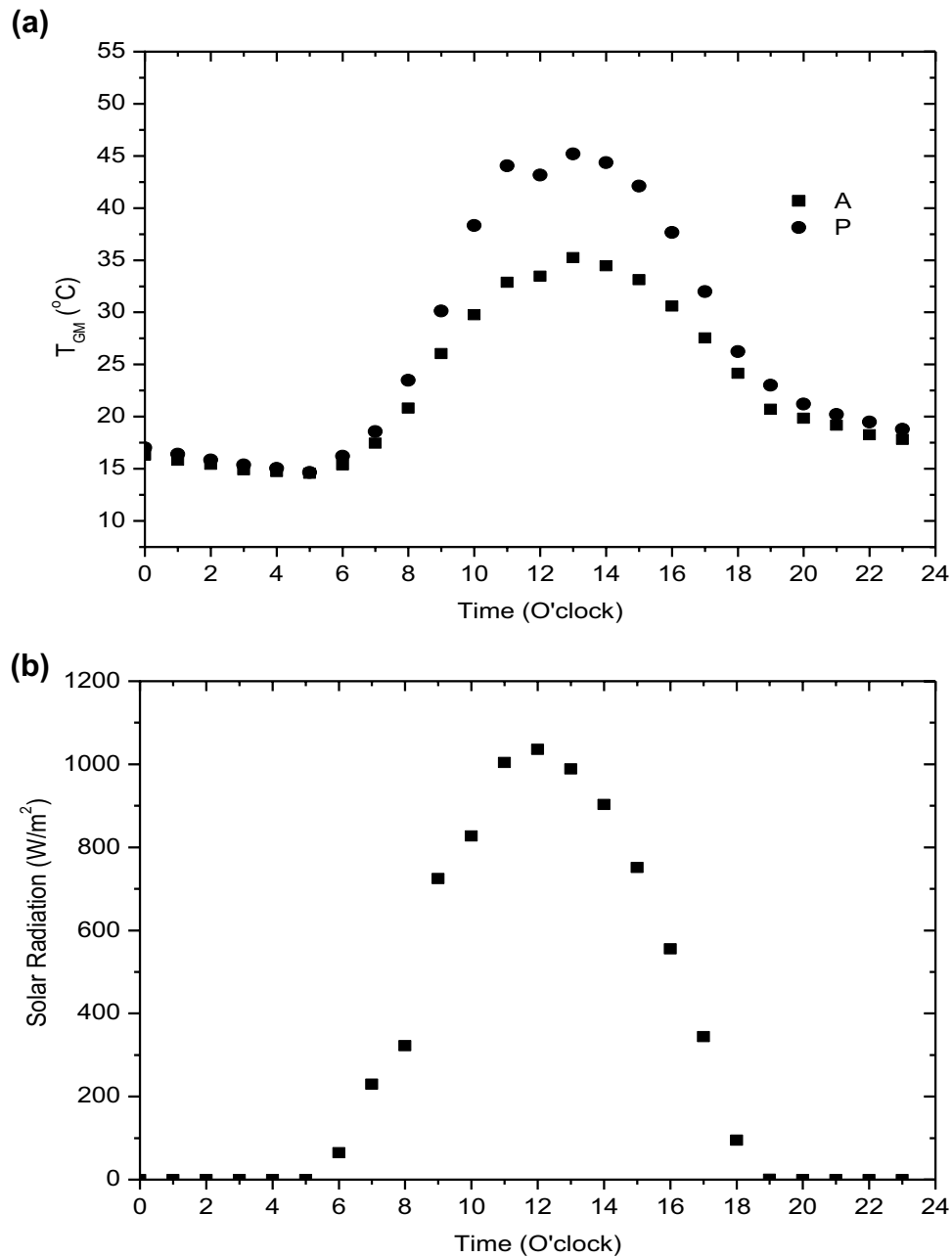


**Figure 5:** GMB temperature and solar radiation **a** GMB temperature collected by probe A and P **b** solar radiation variation within a day. Note: GMB temperature and solar radiation variations were collected on 24 November 2009.

GCL replaced the CCL in the top 7 m to the crest of the slope (Fig. 2).

A total of 15 temperature probes (Figs. 2 and 3 and Table 1) were placed either under or on top of the GMB liner during the construction stage, which lasted from November 2009 to February 2010. In addition, a weather station was installed next to the landfill cell to monitor solar

radiation and air temperature. The logging of all the data commenced on 23 November 2009.

All the temperature sensors were placed in an HDPE pocket glued onto the GMB liner with SikaBond<sup>®</sup>, a high-strength multipurpose adhesive; Fig. 4 shows a thermocouple being installed into an HDPE pocket. The purpose of the HDPE pocket was to ensure that the

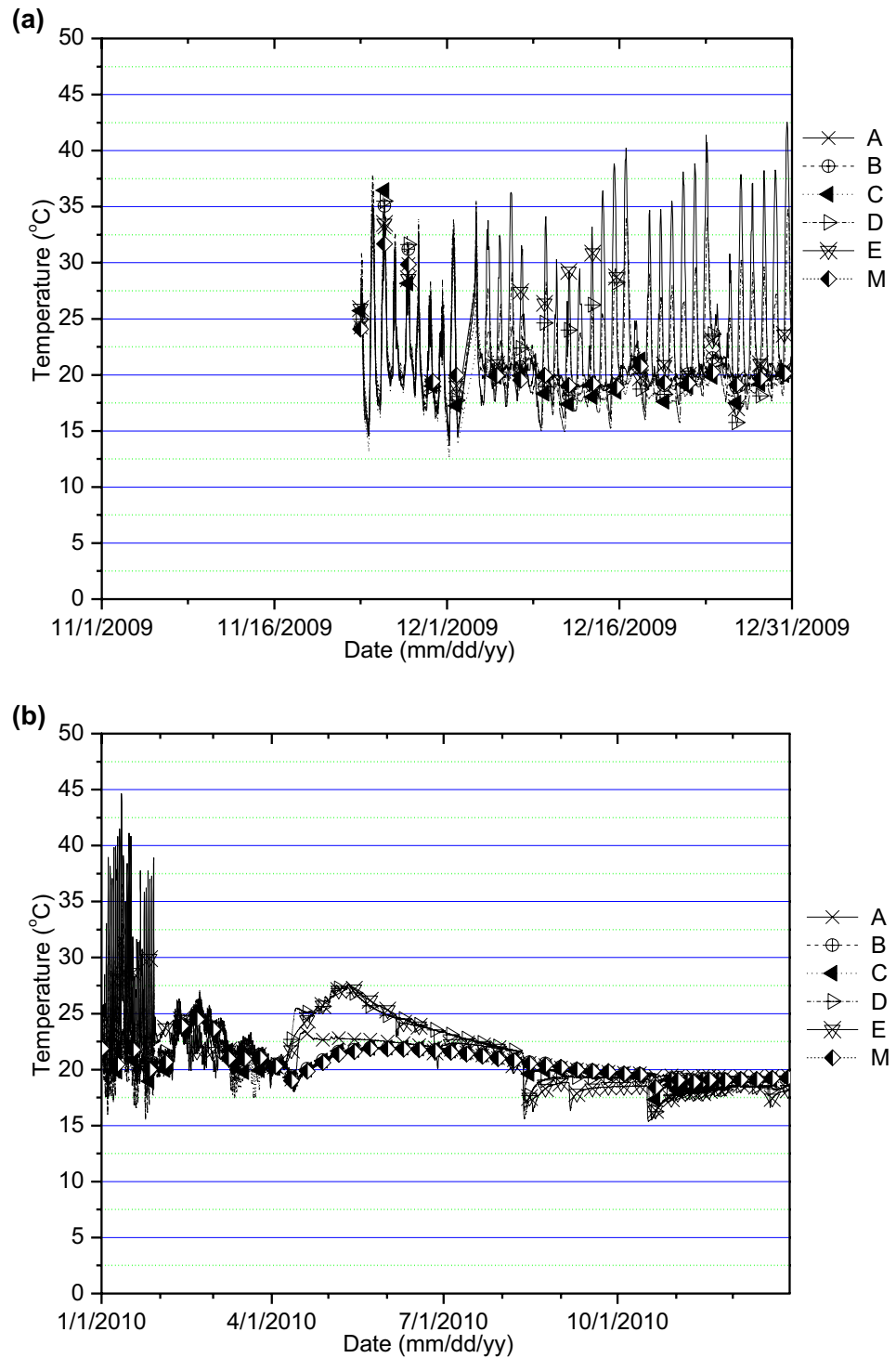


**Figure 6:** Geomembrane temperatures collected from **a** 2009 to **b** 2010 at floor level.

probes were protected against possible exposure to water and/or leachate and record temperature across the HDPE GMB only and not the temperature at the CCL-GMB interface. Furthermore, the thermocouple locations were duplicated in some cases, as shown in Table 1.

### 3 Results and Discussion

The construction of the liner system started in October 2009. The landfill cell started operation in April 2010 and was closed in September 2015. Data has been collected on an hourly basis from 23 November 2009 till November 2016. The



**Figure 7:** Plain view of landfill cell during construction. Note: **a** the red line shows the indicative location of the temperature probes; **b** geomembrane exposed inside the red circle. Photo was taken on 07/01/2010.



**Figure 8:** Plain view of Landfill cell before placement of drainage layer; Note: Photo was taken on 20/02/2010.

maximum and minimum ambient air temperatures recorded on-site were 44 °C and 0 °C on 17 January 2014 and 20 July 2015, respectively (Table 2). It should be noted that the malfunction of some of the sensors occurred due to durability issues, and consequently, some of the data were lost. Therefore, only validated data are presented herein.

*Geomembrane temperature during construction* The lining of the landfill cell was completed on 6 November 2009. The temperature logging started on 23 November 2009, after the geomembrane was covered by a white cushion geotextile. Figure 5 shows the GMB temperature and solar radiation variation on 24 November 2009 at two locations. Temperature variations are reported for probe A located on the geomembrane on the floor of the cell and probe P located on the geomembrane on the slope towards the crest (see

Fig. 2). As shown in Fig. 5, solar radiation plays a vital role in the change of temperature in the geomembrane. For instance, at 1:00 a.m. on 24 November 2009, the solar radiation recorded on site was 0 W/m<sup>2</sup>, and the ambient temperature was 12 °C<sup>34</sup>. The GMB temperature at locations A and P was about 15 °C, indicating that without solar radiation, the temperature of the GMB is very similar to the ambient temperature, with an approximately 3 °C variance. On the same day, at 13:00, the solar radiation reached 1000 W/m<sup>2</sup>, and the ambient temperature was 21 °C. The GMB temperature at location A and P was 35 °C and 46 °C; the temperature is higher at location P due to the slope exposure. Furthermore, the GMB temperature was 14–25 °C higher than the ambient temperature reinforcing the fact that the GMB temperature was more affected by the change of solar radiation strength than ambient temperature. More interestingly, the presence of a white cushion geotextile ( $M_A=700$  g/cm<sup>2</sup> on the floor and  $M_A=500$  g/cm<sup>2</sup> on the side wall) did not alleviate the large swings of temperatures on the GMB caused by solar radiation changes between night and daytime temperature, indicating its incapacity to shield the GMB from temperature variations in exposed situations.

The temperature data collected before 1 December 2009 also shows that most of the other probes, at floor level, followed the same trend (Fig. 6a); the temperature range of the GMB was 15–17 °C at night and 32–42 °C at 13:00 (usually at the peak of solar radiation).

The drainage layer installation on the floor of the site started around 8 December 2009 (Fig. 7a). Its placement had an immediate effect on the temperature ranges recorded on the GMB. The

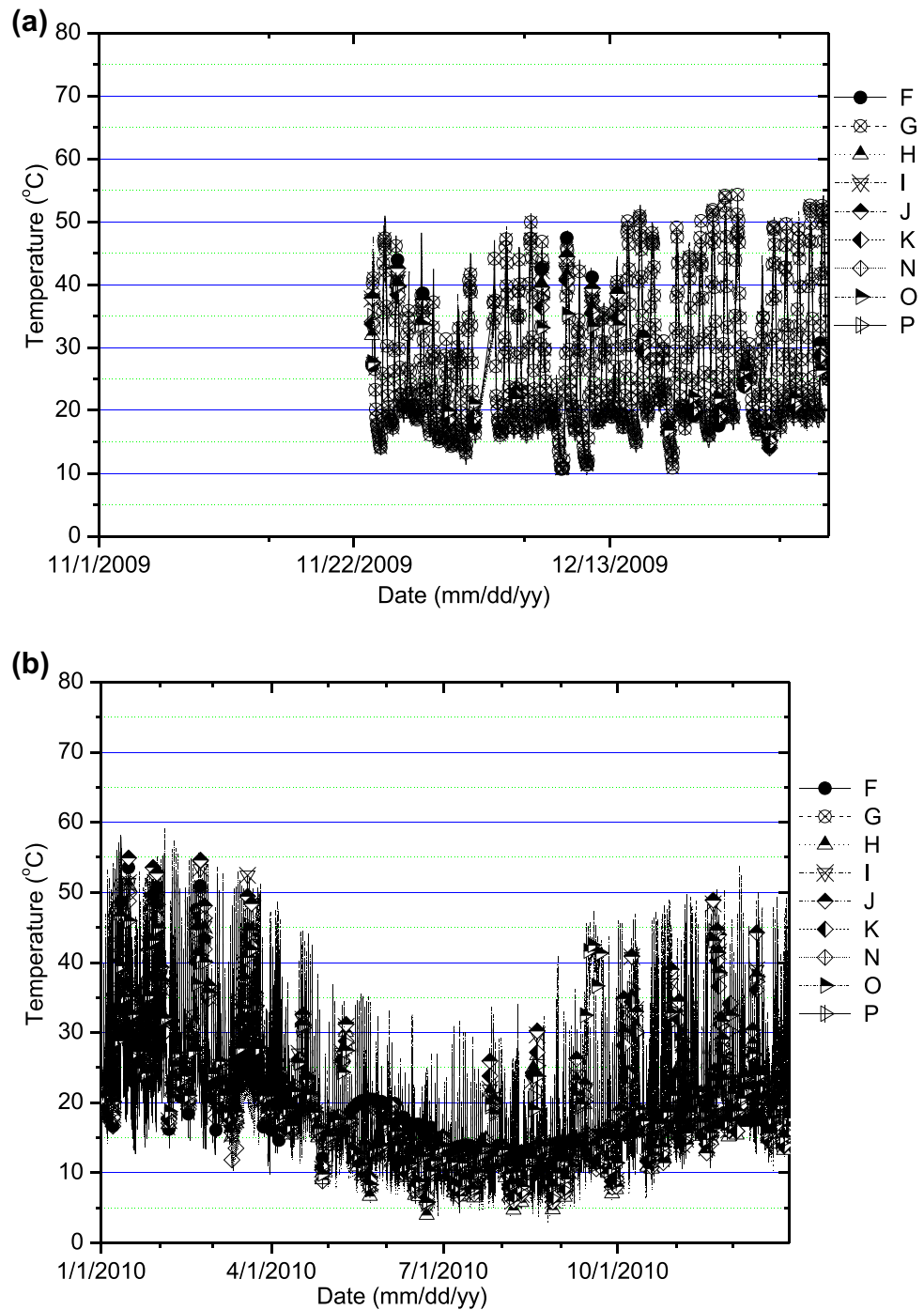


**Figure 9:** Geomembrane temperatures collected from **a** 2009 to **b** 2010 along the side wall.

temperatures at location A, B, C and M fluctuated from 20 to 25 °C (Fig. 6b), which was lower than the GMB temperature fluctuation range 15–38 °C recorded before December 2009. At location D and E, the GMB temperature fluctuation range dropped to 20–25 °C only in February 2010 (Fig. 6b), three months later than the change of the GMB temperature fluctuation range at

location A, B, C, and M. This is due to the end of the year holiday season as the GMB at location D, and E was left uncovered (Fig. 7b, probe D and E are within the circled area). This observation indicates that installing a drainage layer can effectively reduce the impact of solar radiation and shield the geomembrane from heating up to elevated temperatures. Furthermore, it highlights

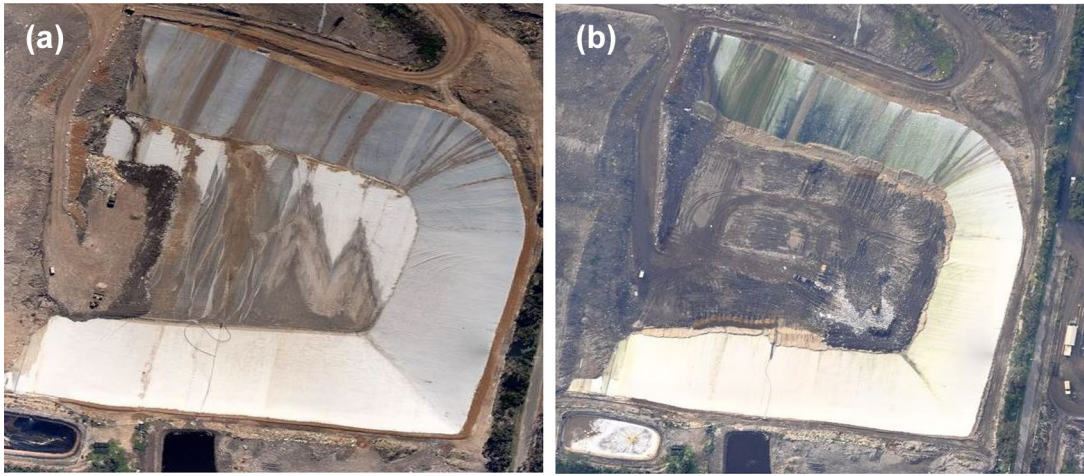


**Figure 10:** Plain view of Landfill cell in April 2010 and June 2010 Note: photos were taken on 16/04/2010 (left) and 22/06/2010 (right).

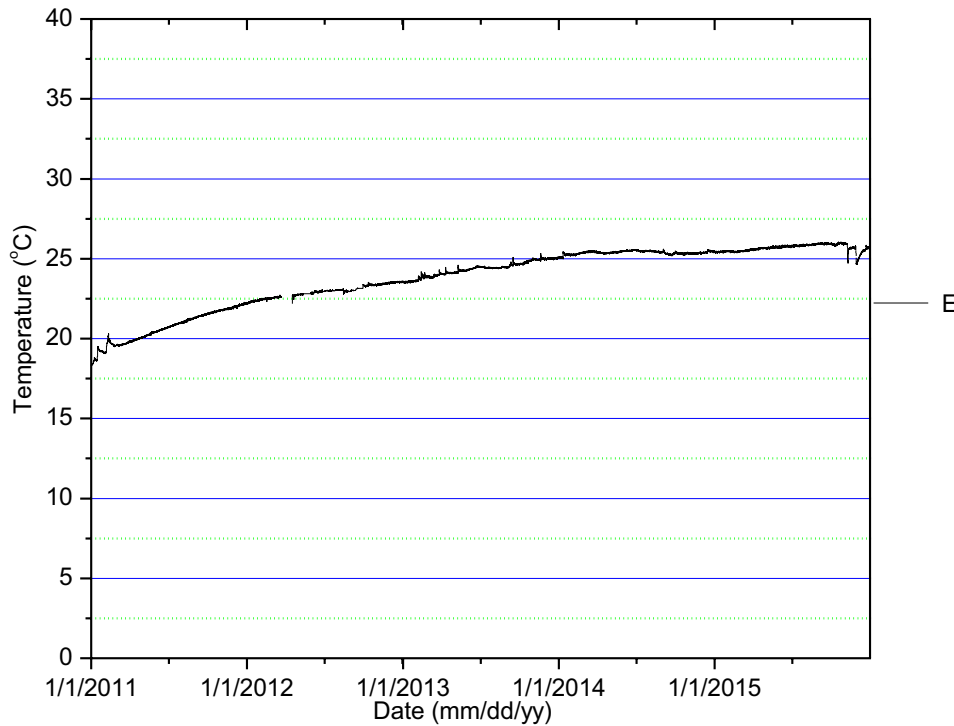


**Figure 11:** Geomembrane temperatures collected from January 2011 to December 2015 at floor level; only probe E was operational.

the fact that the activities on site can also impact the fluctuations of temperatures recorded on geomembranes.

The construction of the liner system was completed in February 2010. Figure 8 shows the whole site covered with a white protective geotextile before installing the drainage layer. During

construction, the maximum temperature experienced by probe A and B was 35 °C and 38 °C, which occurred at 13:00 on 24 November 2009 (Table). Similarly, the maximum temperature recorded by the other probes at floor level varied between 32 °C and 37 °C. In contrast, the maximum GMB temperature along the side slope

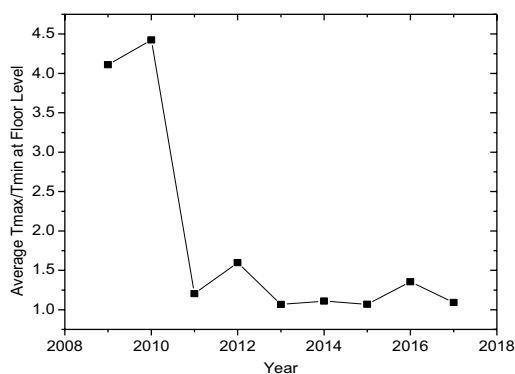


**Figure 12:** Annual geomembrane average temperature ratio at floor level.

ranged between 52 and 59 °C (Table 2 and Fig. 9). The GMB temperature along the side slope was generally higher than the GMB temperature at the floor level, indicating that the GMB temperature at an inclined surface is higher than the GMB temperature on a plain surface when all other conditions are equal.

*Geomembrane temperatures during operation and after cell closure* The landfill cell started operation in April 2010. As observed in Fig. 10, the placement of the soil drainage layer and waste started from the bottom level. In September 2010, the GMB temperature at locations A, B, C, and M peaked at approximately 20 °C and stayed relatively constant for the rest of the year (Fig. 6b). However, the GMB temperature at location D and E reached a relatively stable condition only at the end of 2010 (Fig. 6b). This is likely because waste covered location A, B, C and M first, then location D and E.

Unfortunately, most probes at the floor level failed at the end of 2011, except for probe E, most likely due to the waste placement process. From 2011 to 2015, the GMB temperature recorded by probe E gradually increased from approximately 19–26 °C (Fig. 11) due to the waste biodegradation process. Similar observations on the effect of temperature-induced biodegradation were reported by Yesiller and Hanson<sup>32</sup>, Rowe<sup>24</sup>, Koerner and Koerner<sup>21</sup>, and Bouazza et al.<sup>8</sup>. The annual temperature gradient of the GMB from 2011 to 2015, shown in Fig. 12, indicates that the ratio of the average maximum temperature ( $T_{max}$ ) to the average minimum temperature ( $T_{min}$ ) recorded at floor level decreased over time and reached approximately one. Thus, the maximum change of the temperature of the GMB occurred in the first year of operation after the placement of the waste.

On the side slope, the temperatures were dependent on the rate of filling and drainage installation. If one looks, for example, at location J (25 m down from the slope crest, Fig. 2), before December 2011, the GMB temperature fluctuated between 5 and 60 °C daily (Fig. 13), until the GMB was covered at this location. Then temperature became relatively constant at the 22–25 °C range. Along the side wall, the GMB temperature at location F and N reached a relatively stable condition from May 2010 (Table 3). This was due to the placement of the drainage layer, highlighting its importance in minimising solar radiation. Similar observations could also be made for locations G, H, I, J, K, O and P (Table 3). The order of each probe to reach a relatively stable condition was related to its location. As shown in Table 3, the thermocouple installed further away from the crest of the slope (probe F, 55 m from the crest of the slope) reached a stable condition before the one installed close to the crest (probe K, 15 m from the crest of the slope) because the site was gradually filled up. This is also illustrated by the aerial images shown in Fig. 14. Before the site's closure, the GMB temperature recorded by the probes along the side wall ranged from 20 to 25 °C at an increasing rate of approximately 1 °C per annum.

The landfill site was closed in September 2015. The change of the GMB temperature after the closure of the site was approximately 1 °C. The GMB temperature at the floor level was approximately 26 °C (Fig. 15); whereas, on the side wall it was approximately 23 °C except at location F, where temperature decreased from 23 to 20 °C (Fig. 16).

As discussed earlier, the temperature of the GMB fluctuated with the intensity of solar radiation. Figure 17 summarises the variation of solar radiations from Nov. 2009 to August 2010 on the side wall slope, which was fully exposed. The corresponding difference between the temperature recorded on the geomembrane and the ambient temperature is shown in Fig. 18 for probe J only (similar variations were observed for the other probes on the slope). For example, in summer, the intensity of solar radiation peaked at 1350 W/m<sup>2</sup>, resulting in the GMBs temperature being 30 °C higher than the ambient air temperature. In winter, the intensity of solar radiation decreased to about 100–400 W/m<sup>2</sup> resulting in the GMB temperature being 10–20 °C higher than the ambient temperature.

A theoretical relationship between solar radiation and fully exposed GMBs temperature was developed by Pelte et al.<sup>23</sup> and is expressed as:

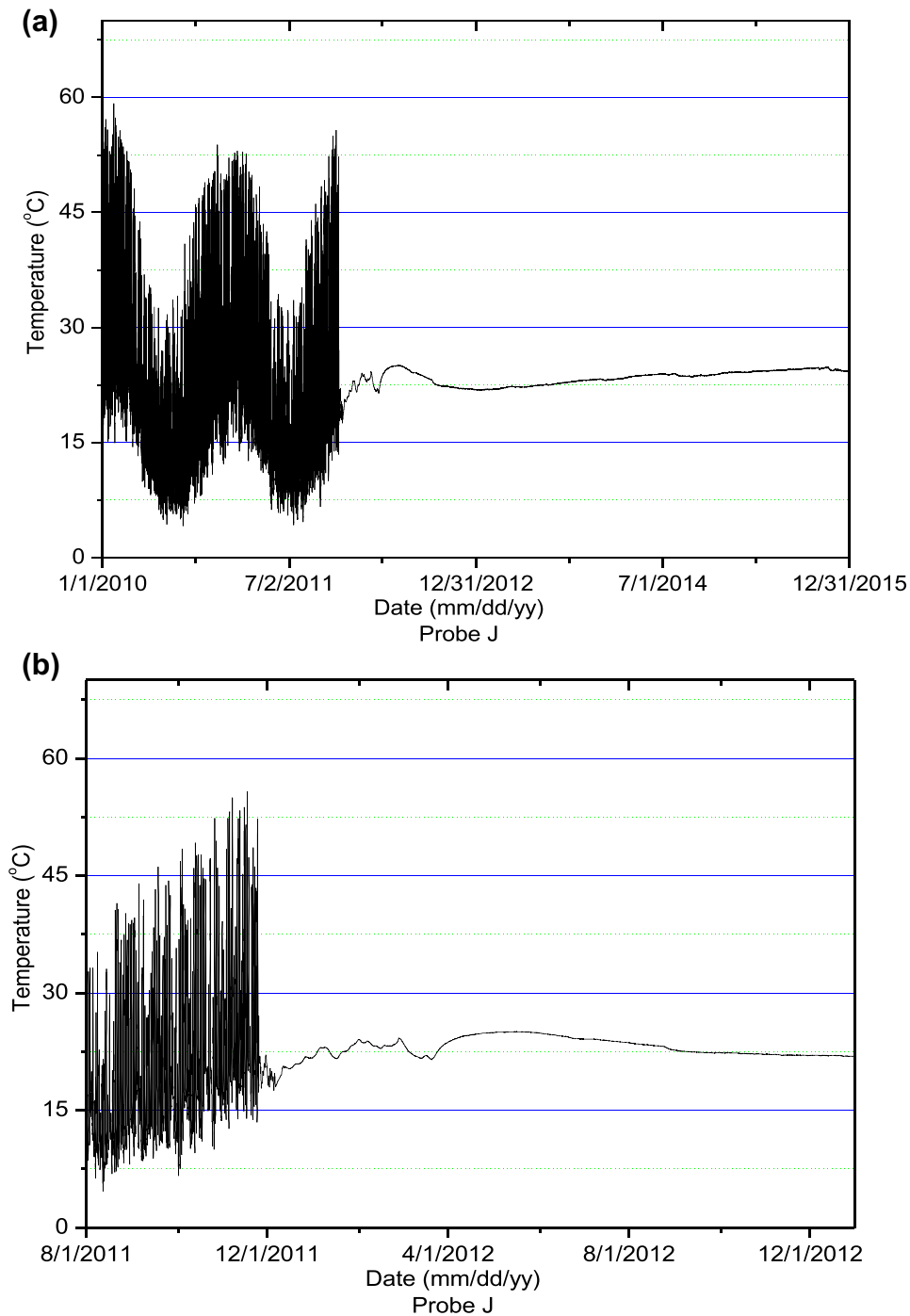


**Figure 13:** Temperature of geomembrane at location J. Note: **a** shows the temperature change at location J from 2010 to 2015 **b** shows the detailed temperature change at location J after the placement of drainage layer and waste.

$$\alpha G = h(T_{GM}(t) - T_a + (x = 0, t) + \mu_{GM} C_P \frac{dT_{GM}(t)}{dt}, \quad (1)$$

where  $\alpha$  is the solar energy absorption coefficient,  $G$  ( $W/m^2$ ) is the total solar energy per unit area acting on the plane of the GMB,  $h$  is the heat exchange coefficient (which depends on wind speed) ( $W/m^2/^\circ C$ ),  $T_{GM}$  ( $^\circ C$ ) is the surface

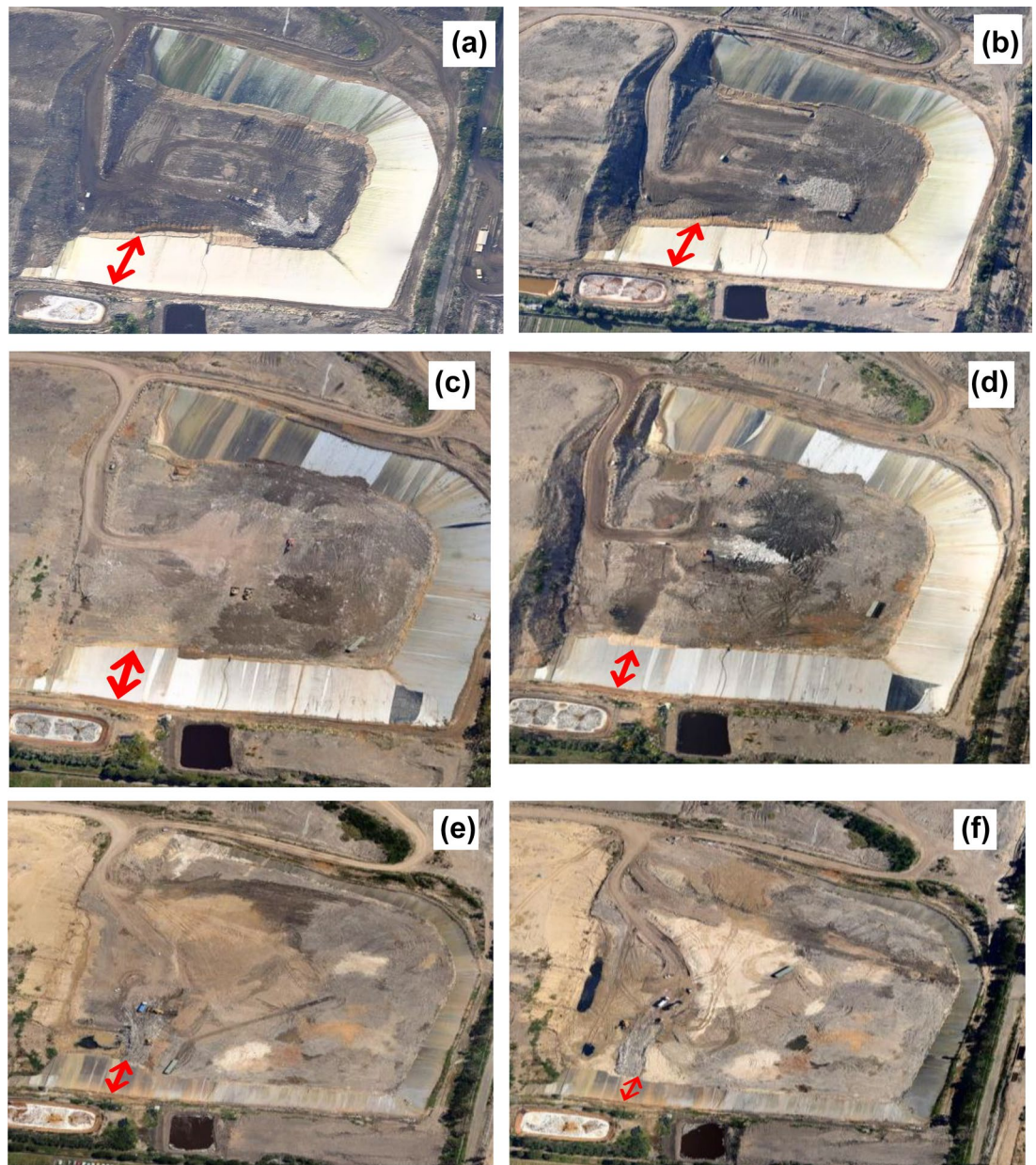


**Figure 14:** Aerial view of Landfill cell from July 2010 to December 2011. Note: photos were taken on 11/07/2010 **a**, 03/10/2010 **b**, 20/10/2010 **c** 24/12/2010 **d** 17/11/2011 **e** 05/12/2011 **f**.

temperature of the GMB which varies with time  $t$ ,  $T_a$  ( $^{\circ}\text{C}$ ) is the ambient air temperature,  $\Phi$  ( $\text{W}/\text{m}^2$ ) is the heat flux in the soil per unit area,  $\mu_{\text{GM}}$  ( $\text{kg}/\text{m}^2$ ) is the mass per unit area of the GMB,  $C_p$  ( $\text{J}/\text{kg}^{\circ}\text{C}$ ) is the specific heat of soil, and  $x$  is the vertical distance below the surface of the GMB.

Brachman et al.<sup>12</sup> indicated that the temperature of the interface between a GMB and a mineral liner depended on the solar radiation and the ambient air temperature, with additional minor effects from the temperature of the underlying soil (i.e. subgrade). Thus, Eq. 1 is simplified to

Eq. 2, rearranging Eq. 2 gives the theoretical  $T_{\text{GM}}$  shown in Eq. 3:

$$\alpha G = h(T_{\text{GM}}(t) - T_a), \quad (2)$$

$$T_{\text{GM}}(t) = \frac{\alpha G}{h} + T_a, \quad (3)$$

$T_a$  and  $G$  were measured on site.  $\alpha$  is dependent on the colour of the material because of emissivity<sup>23</sup>. Pelte et al.<sup>23</sup> indicated that  $\alpha$  for a black GMB is 1 and the  $\alpha$  for a white geotextile

**Table 3:** Time for temperature probes to reach a stable temperature.

Sensor	Floor level		Sensor	Side wall	
	Cable length (m)	Stable temp reached at		Cable length (m)	Stable temp reached at
A	108	Dec 2009	F	55	May 2010
M	104	Dec 2009	N	53	May 2010
B	98	Dec 2009	G	45	Jul 2010
C	88	Dec 2009	H	35	Mar 2011
D	78	Feb 2010	O	34	Mar 2011
E	66	Feb 2010	I	25	Dec 2011
			J	25	Dec 2011
			P	23	Dec 2011
			K	15	Mar 2012

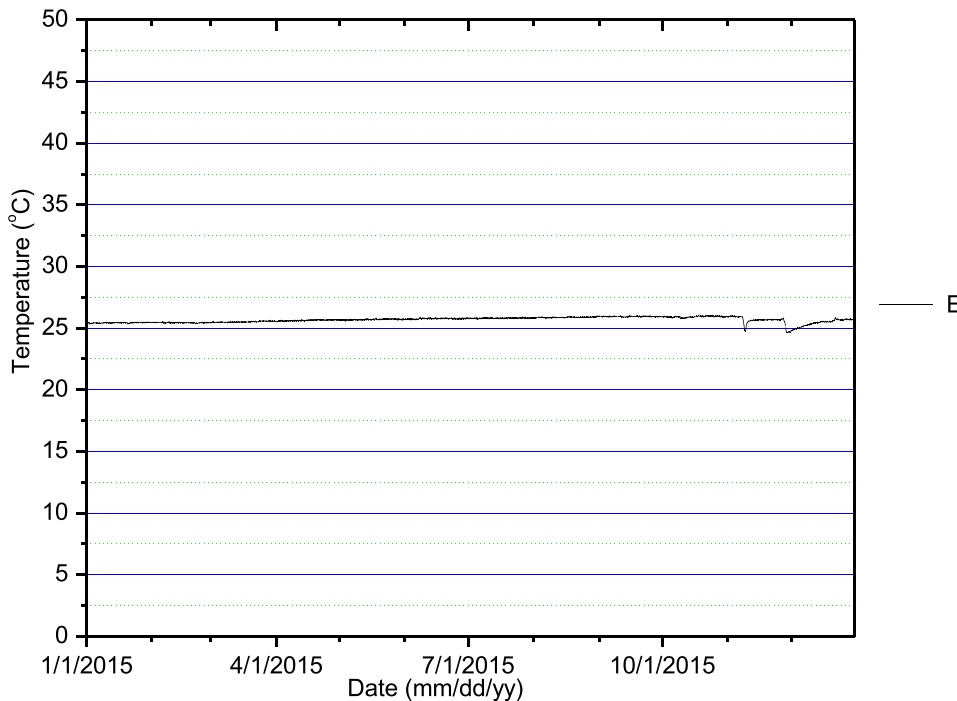


**Figure 15:** Geomembrane temperatures in 2015 at floor level collected, only probe E was still operational.

is  $0.7 \pm 0.2$ . As the black GMB placed along the side wall was covered by a white cushion geotextile, the  $\alpha$  in this case is assumed to be between 0.5 and 1. Pelte et al.<sup>23</sup> indicated that the heat exchange coefficient in the vertical direction  $h_v$  (vertical) is  $8 \pm 2 \text{ Wm}^{-2} \text{ }^\circ\text{C}^{-1}$  and in the horizontal direction  $h_h$  (horizontal) is  $13 \pm 1/\text{Wm}^2/^\circ\text{C}$ . Therefore, the maximum  $h_v$  and  $h_h$  are  $10/\text{Wm}^2/^\circ\text{C}$  and  $14 \text{ /Wm}^2/^\circ\text{C}$ , and the minimum  $h_v$  and  $h_h$  are  $6 \text{ Wm}^{-2}\text{ }^\circ\text{C}^{-1}$  and  $12 \text{ Wm}^{-2} \text{ }^\circ\text{C}^{-1}$ . Since the land-fill slope is 3H:1 V, directly applying the  $h_v$  and

$h_h$  provided by Pelte et al.<sup>23</sup> to this case study is inappropriate. Therefore, trigonometry was used to find the resultant  $h_r$ . Based on the maximum  $h_v$  and  $h_h$  and the minimum  $h_v$  and  $h_h$  given in Pelte et al.<sup>23</sup>, the  $h_r$  for a 3H:1 V slope is between 10 and 13.

To find the optimised  $\alpha$  and  $h_r$  for a black GMB covered by a white geotextile, it was assumed that the theoretical GMB temperature and the GMB field measured temperature are equal (Fig. 19); thus, a linear relationship between

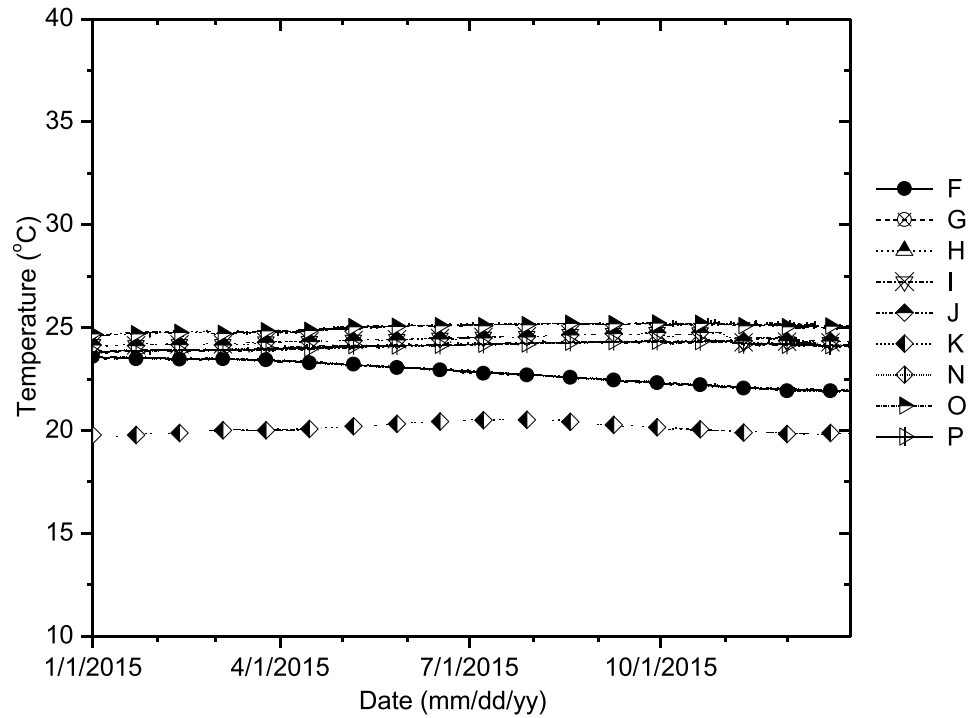


**Figure 16:** Geomembrane temperature collected in 2015 along the side wall.

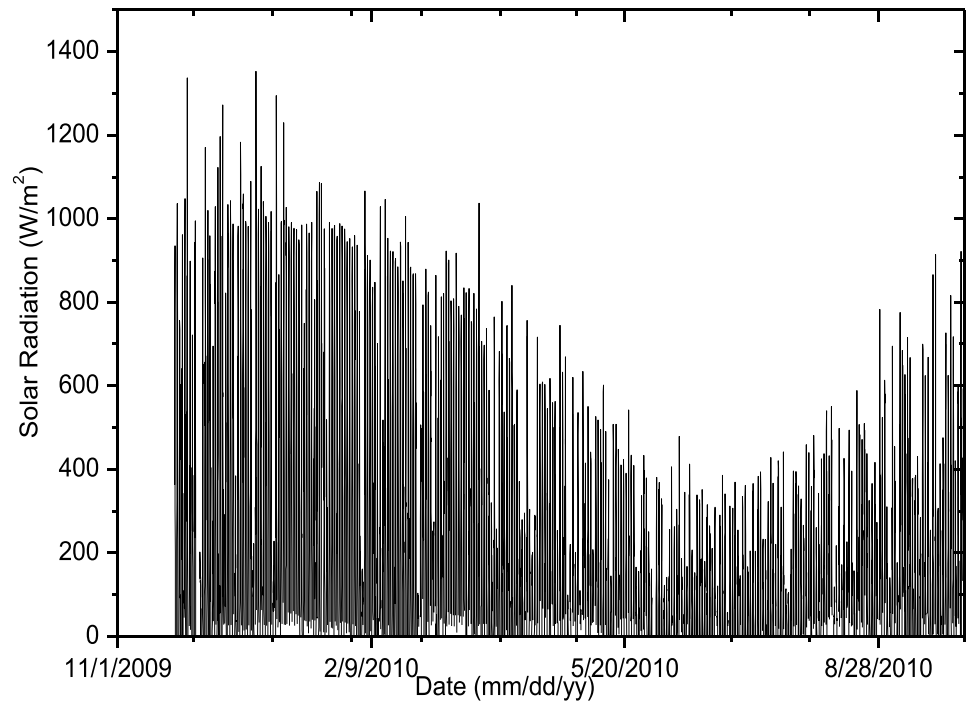


**Figure 17:** Intensity of solar radiation between November 2009 and August 2010.

the two measurements prevails. Probe P was selected to represent the GMB temperature along the side wall. Table 4 shows the variation of the solar energy absorption coefficient  $\alpha$  and heat

exchange coefficient  $h_r$  for different cases. The best fit for the linear relationship represented by the reference line (RL) shown in Fig. 19 is for  $\alpha = 0.5$ ,  $h_r = 13$  with  $R^2 = 0.86$  (note the same

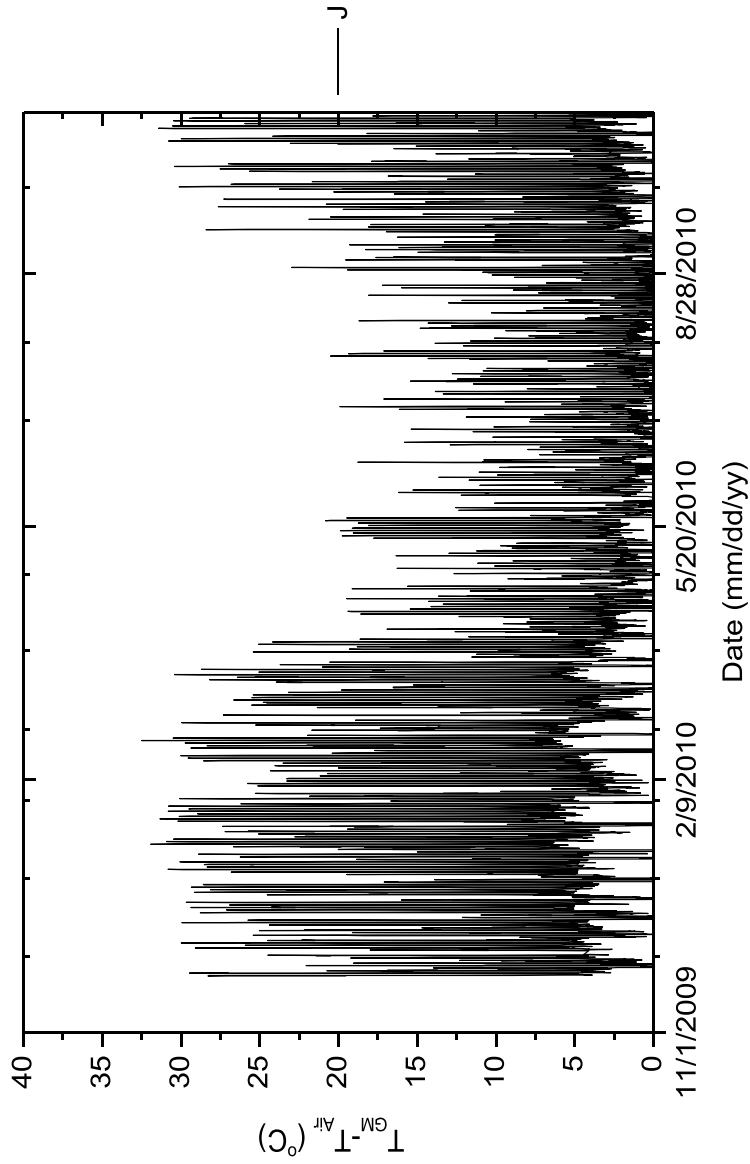


**Figure 18:** Difference between the geomembrane temperature of GMB and the temperature of ambient air between November 2009 and August 2010.

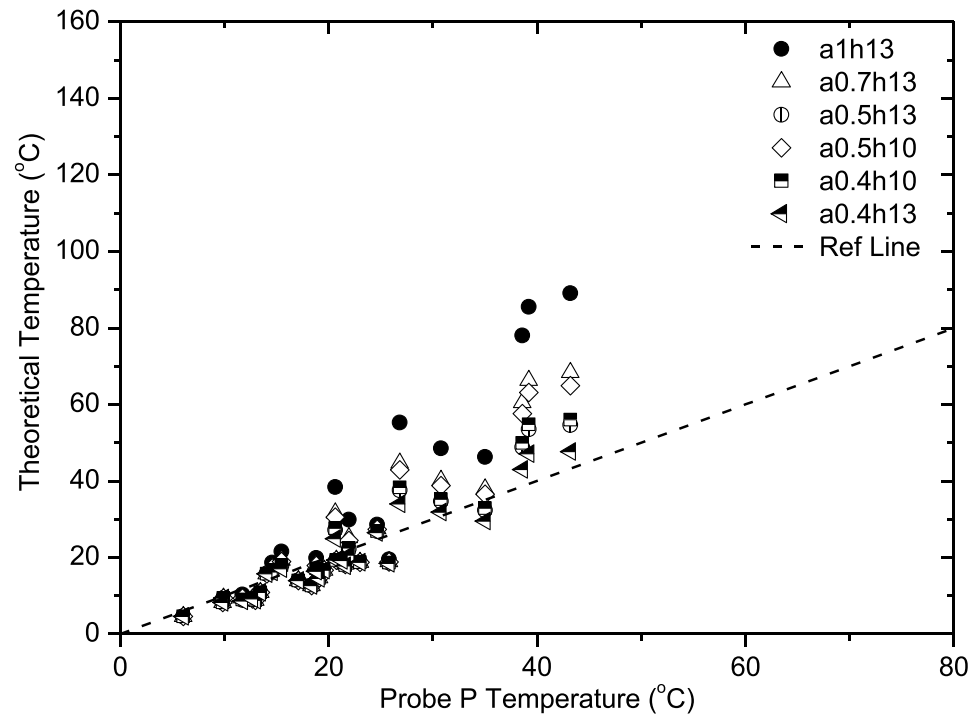


**Figure 19:** Theoretical GMB temperature versus field GMB temperature  $h_r = 13$ . Note: RL is the reference line that the theoretical GMB temperature = field GMB temperature.

process was followed for  $h_r = 10\text{--}12$ ). Thus, for the current site the solar energy absorption coefficient of the GMB is 0.5, and its heat exchange coefficient is  $13/\text{Wm}^2/\text{°C}$ .

#### 4 Conclusions

This study analysed the temperature variations of a black HDPE GMB in a municipal soil waste landfill located in the Southern Hemisphere from construction (the year 2009) to closure (the year 2016) through a monitoring process. The salient conclusions that can be drawn from this study are as follow:

1. Before the placement of a drainage layer, the daily maximum recorded GMB temperature was related to the maximum solar radiation and ambient temperature recorded on the day. The daily minimum GMB temperature was either equal to or slightly higher than the minimum ambient temperature. Solar radiation had a greater impact on an inclined GMB surface temperature than on a plain GMB surface temperature.

2. The placement of a drainage layer can effectively reduce the impact of solar radiation on the GMB and insulate it. In summer, the daily temperature variation of a black GMB covered with a white geotextile varied from 12 to 38 °C at floor level. After the placement of the drainage layer, the temperature of the GMB became stable and dropped to approximately 20 °C. Along the side wall, without the drainage layer, the daily temperature variation of the GMB fluctuated between 5 and 60 °C. After the placement of the drainage layer, the GMB temperature reached a stable condition and remained at approximately 23 °C. This study also showed that relying only on a white geotextile with mass per unit area in the range of 500–700 g/cm<sup>2</sup> will not insulate the geomembrane from the effect of solar radiations and will still experience elevated temperatures.

#### Publisher's Note

Springer Nature remains neutral with regard to jurisdictional claims in published maps and institutional affiliations.



12. Brachman RWI, Rowe RK, Arnepalli DN, Take WA (2015) Thermal exposure conditions for a composite liner with a black geomembrane exposed to solar radiation. *Geosynth Int* 22:93–109. <https://doi.org/10.1680/gein.14.00034>
13. Calder GV, Stark TD (2010) Aluminum reactions and problems in municipal solid waste landfills. *Pract Period Hazardous Toxic Radioact Waste Mana* 14:258–265. [https://doi.org/10.1061/\(ASCE\)HZ.1944-8376.0000045](https://doi.org/10.1061/(ASCE)HZ.1944-8376.0000045)
14. Carnero-Guzman GG, Bouazza A, Gates WP, Rowe RK, McWatters R (2021) Hydration/dehydration behaviour of geosynthetic clay liners in the Antarctic environment. *Geotext Geomembr* 49:196–209. <https://doi.org/10.1016/j.geotextmem.2020.10.020>
15. ENSR (2008) Technical specification Clayton road landfill stage 2. ENSR Australia Pty Ltd (ENSR)
16. Ghavam-Nasir A, El-Zein A, Airey D, Rowe RK, Bouazza A (2019) Numerical simulation of geosynthetic clay liner desiccation under high thermal gradients and low overburden stress. *Int J Geomech* 19:04019069. [https://doi.org/10.1061/\(ASCE\)GM.1943-5622.0001425](https://doi.org/10.1061/(ASCE)GM.1943-5622.0001425)
17. Ghavam-Nasiri A, El-Zein A, Airey D, Rowe RK, Bouazza A (2020) Thermal desiccation of geosynthetic clay liners under brine pond conditions. *Geosynth Int* 27:593–605. <https://doi.org/10.1680/jgein.20.00020>
18. Hanson JL, Yesiller N, Oettle N (2010) Spatial and temporal temperature distributions in municipal solid waste landfills. *J Environ Eng* 136:804–814. [https://doi.org/10.1061/\(ASCE\)EE.1943-7870.0000202](https://doi.org/10.1061/(ASCE)EE.1943-7870.0000202)
19. Jafari NH, Stark TD, Rowe RK (2014) Service life of HDPE geomembranes subjected to elevated temperatures. *J Hazard Toxic Radioact Waste* 18:16–26. [https://doi.org/10.1061/\(ASCE\)HZ.2153-5515.0000188](https://doi.org/10.1061/(ASCE)HZ.2153-5515.0000188)
20. Klein R, Baumann T, Kahapka E, Niessner R (2001) Temperature development in a modern municipal solid waste incineration (MSWI) bottom ash landfill with regard to sustainable waste management. *J Hazard Mater* 83:265–280. [https://doi.org/10.1016/S0304-3894\(01\)00188-1](https://doi.org/10.1016/S0304-3894(01)00188-1)
21. Koerner GR, Koerner RM (2006) Long-term temperature monitoring of geomembranes at dry and wet landfills. *Geotext Geomembr* 24:72–77. <https://doi.org/10.1016/j.geotextmem.2004.11.003>
22. McWatters RS, Rowe RK, Wilkins D, Spedding T, Jones D, Terry D, Hince G, Wise L, Gates WP, Bouazza A, Battista VD, Shoaib M, Snape I (2016) Geosynthetics in Antarctica: performance of a composite barrier system to contain hydrocarbon-contaminated soil after 3 years in the field. *Geotext Geomembr* 44:673–685. <https://doi.org/10.1016/j.geotextmem.2016.06.001>
23. Pelte T, Pierson P, Gourc JP (1994) Thermal analysis of geomembrane exposed to solar radiation. *Geosynth Int* 1:21–44. <https://doi.org/10.1680/gein.1.0002>
24. Rowe RK (2005) Long-term performance of contaminant barrier systems. *Geotechnique* 55:631–678. <https://doi.org/10.1680/geot.2005.55.9.631>
25. Rowe RK, Chappel MJ, Brachman RWI, Take WA (2012) Field study of wrinkles in a geomembrane at a composite liner test site. *Can Geotech J* 49:1196–1211. <https://doi.org/10.1139/t2012-083>
26. Rowe RK, Islam MZ (2009) Impact of landfill liner time-temperature history on the service life of HDPE geomembranes. *Waste Manag* 29:2689–2699. <https://doi.org/10.1016/j.wasman.2009.05.010>
27. Singh RM, Bouazza A (2013) Thermal conductivity of geosynthetics. *Geotext Geomembr* 39:1–8. <https://doi.org/10.1016/j.geotextmem.2013.06.002>
28. Take WA, Watson E, Brachman RWI, Rowe RK (2012) Thermal expansion and contraction of geomembrane liners subjected to solar exposure and backfilling. *J Geotech Geoenviron Eng* 138:1387–1397. [https://doi.org/10.1061/\(ASCE\)GT.1943-5606.0000694](https://doi.org/10.1061/(ASCE)GT.1943-5606.0000694)
29. Tincopa M, Bouazza A (2021) Water retention curves of a geosynthetic clay liner under non-uniform temperature-stress paths. *Geotext Geomembr*. <https://doi.org/10.1016/j.geotextmem.2021.04.005>
30. Touze-Foltz N, Xie H, Stoltz G (2021) Performance issues of barrier systems for landfills: a review. *Geotext Geomembr* 49:475–488. <https://doi.org/10.1016/j.geotextmem.2020.10.016>
31. Touze-Foltz N, Bannour H, Barral C, Stoltz G (2016) A review of the performance of geosynthetics for environmental protection. *Geotext Geomembr* 44:656–672. <https://doi.org/10.1016/j.geotextmem.2016.05.008>
32. Yesiller N, Hanson JL (2003) Analysis of temperatures at a municipal solid waste landfill. In: Christensen et al. (ed) . *Sardinia 2003*, Ninth International Waste Management and Landfill Symposium. CISA, Italy, pp 1–10
33. Yesiller N, Hanson J, Liu W (2005) Heat generation in municipal solid waste landfills. *J Geotech Geoenviron Eng* 131:1330–1344. [https://doi.org/10.1061/\(ASCE\)1090-0241\(2005\)131:11\(1330\)](https://doi.org/10.1061/(ASCE)1090-0241(2005)131:11(1330))
34. Zhang L (2018) Durability of HDPE geomembranes to leachates of extreme chemistry, PhD Thesis, Monash University, Melbourne, Australia.
35. Zhang L, Bouazza A, Rowe RK, Scheirs J (2017) Effect of welding parameters on properties of HDPE geomembrane seams. *Geosynth Int* 24:408–418. <https://doi.org/10.1680/jgein.17.00011>
36. Zhang L, Bouazza A, Rowe RK, Scheirs J (2018) Effects of a very low pH solution on the properties of an HDPE geomembrane. *Geosynth Int* 25:118–131. <https://doi.org/10.1680/jgein.17.00037>



**Abdelmalek Bouazza** is a professor of civil engineering at Monash University. He has an international reputation for research in geosynthetics and environmental geotechnics. His research has been recognised by numerous national and international awards. Professor Bouazza is very prominent in technical and professional society activities and serves on a number of international technical committees. Currently, he is the chair of the International Soil Mechanics and Geotechnical Engineering (ISSMGE) Technical Committee TC 215 on Environmental Geotechnics. In addition to his academic commitments, Dr Bouazza gives specialist advice for the industry both nationally and internationally. His work has included peer review of design for more than 30 municipal solid waste and hazardous landfills and tailings storage facilities in Australia, Thailand, Peru and other countries. He has led and co-wrote the key line components of the

landfill standard for the State of Victoria (Best Practice Environmental Management: Siting, design, operation and rehabilitation of landfills, EPA Publication 788), which is now used as a model for much of the country.



**Lu Zhang** graduated with a PhD in civil engineering from Monash University in 2017 after completing a bachelor of engineering (BEng) in civil engineering also at Monash University in 2012. Dr Lu is currently a geotechnical engineer at Cardno Victoria Pty Ltd., Melbourne, Australia, where she specialises in site investigation, numerical and geotechnical analysis, and tendering and project management. She has been involved in a number of projects including major road upgrades, wind farm pavements, rehabilitation and level crossing removal and other projects related to environment protection.